

Measurements of Stimulated-Raman-Scattering Instability Relevant to Ignition Hohlraum Plasmas

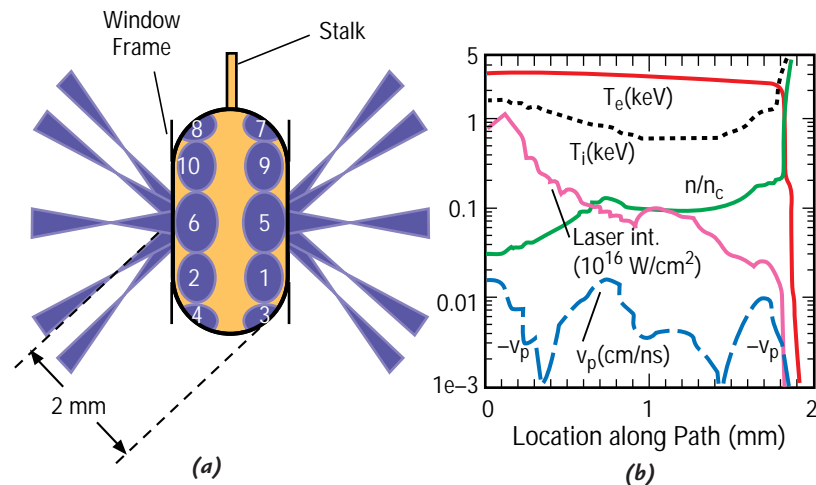
J. C. Fernández, B. S. Bauer,
J. A. Cobble, G. A. Kyrala,
D. S. Montgomery, R. G. Watt,
M. D. Wilke (P-24),
W. M. Wood (P-22),
D. F. DuBois, H. A. Rose (T-13),
H. X. Vu (XPA),
B. H. Wilde (XTA),
B. H. Failor (Physics International, San
Leandro, California), R. Kirkwood,
B. J. MacGowan (Lawrence Livermore
National Laboratory)

Introduction

Control of laser-plasma instability is important for the success of laser fusion,¹ particularly indirect drive.² For indirect drive, laser beams enter a cavity (called a hohlraum) made of a material that has a high atomic number and that reaches a high ionization state (high Z). The high- Z plasma efficiently converts laser energy into x-rays, which in turn drive the implosion of a fusion capsule. Ignition hohlraums, such as those planned for the National Ignition Facility (NIF),² are expected to contain underdense plasmas (a few millimeters in size) with electron temperatures (T_e) in the kiloelectronvolt range. Present NIF hohlraum designs rely on the plasma pressure from a helium-hydrogen gas fill to tamp intrusion into the hohlraum volume by the gold-wall plasma, while allowing laser propagation inside the hohlraum.³ Thus, the longest scale lengths are expected to be within the low- Z helium-hydrogen plasma.

Because scientists lack a fundamental understanding of many aspects of laser-plasma instabilities, it is desirable to study these instabilities in plasma conditions that are as close as possible to those expected in NIF hohlraums. Radiation-hydrodynamic simulations of NIF hohlraums⁴ with the LASNEX code⁵ (an inertial confinement fusion [ICF] design code) indicate that a variety of plasma conditions will exist within the NIF hohlraum. Not all of these conditions can be studied. Both inspection and postprocessing of LASNEX simulations of NIF hohlraums⁶ show that it is clearly worth considering the millimeter-scale plasmas, with low Z , $n_e / n_c \approx 0.1$, and $T_e \approx 3\text{--}5$ keV expected in NIF-hohlraum plasmas (n_e is the electron density and n_c is the critical density above which the laser's light cannot propagate). Present lasers cannot reproduce all of the required conditions simultaneously, but they can approach the conditions so that useful data can be obtained.

Fig. II-20. (a) An illustration of the gas-filled hohlraum. The footprints of the 10 Nova beams incident on the inner wall are indicated; those on the far wall have a dashed outline. (b) Calculated profiles within the hohlraum along a beam path (starting at the laser entrance hole) are plotted for a time of 1 ns.



Plasma Conditions

In this article we discuss the results obtained with toroidally shaped hohlraums,^{7,8} which approach NIF conditions when illuminated with the Nova laser at Lawrence Livermore National Laboratory.⁹ These targets were designed by X Division and fabricated by MST Division, and the experiments were fielded by P-Division scientists at Los Alamos. An illustration of the hohlraum is shown in Fig. II-20, reproduced from Fig. 1 of Ref. 7. It is cylindrically symmetric with a length of 1.6 mm and a diameter of 3.2 mm. All 10 laser beams operate at a wavelength of 351 nm. In the toroidal hohlraum we have used various gas fills, contained by thin, 0.3- μ m-thick silicon nitride windows covering the laser entrance hole (LEH). Typical fills are low-Z gases such as C₅H₁₂, C₅D₁₂, CF₄, and CF₄ + C₅H₁₂ mixtures at 1 atm of pressure, designed to fully ionize to $n_e / n_c = 0.11$. They span the range $Z_{\text{eff}} = 2.5\text{--}8$. The calculated spatial profiles of n_e , T_e , T_i , and plasma-flow speed (v_p) along the direction of laser propagation (\hat{k}_0) for C₅H₁₂ are also shown in Fig. II-20. For C₅H₁₂, $T_e = 3$ keV has been measured,^{7,8} which is in agreement with LASNEX simulations. From Fig. II-20, the scale lengths for density, $L_n \equiv n_e / (\hat{k}_0 \cdot \nabla n_e)$, and velocity, $L_v \equiv c_s / (\hat{k}_0 \cdot \nabla v_p)$ are similar ($L_n \approx L_v \approx 1\text{--}2$ mm). In the latter definition c_s is the ion-acoustic speed.

Laser-Plasma Instability

In the long-scale NIF plasmas, high levels of laser-plasma instability are predicted by linear convective theory.¹⁰ Stimulated Raman scattering (SRS)¹¹ and stimulated Brillouin scattering (SBS),¹² in particular, could be significant. SRS and SBS involve scattering of laser light by electron-plasma (Langmuir) waves and ion-acoustic waves, respectively. From the initial noise level, these unstable waves would develop a growing amplitude in space. The backscattering direction is expected to have the highest spatial gain. The calculated gains from linear theory, even assuming smooth laser beams, are generally enormous ($\exp[25]\text{--}\exp[30]$) in plasmas such as ours,⁶ and nonlinear saturation mechanisms are expected to occur. The high-energy glass-laser beams used for ICF are not spatially uniform. They have a broad distribution of intensities about the average value. Without any beam modification, these nonuniformities appear mostly as relatively large scale spatial fluctuations, with dimensions nonnegligible relative to the beam diameter.¹³ Spatial smoothing can be accomplished with a binary random-phase plate (RPP),¹⁴ which breaks the raw beam into smaller beamlets with a random 0 or π phase delay. RPPs produce a spatially “smooth” focal spot envelope with a superimposed fine-scale speckle (or “hot spot”) pattern. The statistics of RPP hot spots are well known,¹⁵ and it is clear that a significant fraction of the beam energy is tied up in hot spots. The known RPP hot-spot statistics allow better theoretical modeling of SBS and SRS in real plasmas, which recently has been successfully done by T-Division scientists.

SRS Onsets

We have verified that laser hot spots change the character of SRS and SRS instability onsets relative to theoretical predictions for smooth beams. With smooth beams, convective amplification of thermal density fluctuations would yield an SRS reflectivity that depends exponentially on laser intensity and L_n (\approx plasma size). But in the fluid model in Ref. 16, which is applicable to SRS and SRS in NIF conditions, instability gain on hot spots is computed including effects such as beam diffraction and pump depletion. Including diffraction is important because it can significantly decrease the spatial gain within a hot spot when the beam f -number is moderately small.^{16,17} When the results are integrated over the RPP hot-spot distribution, the system becomes nonlinear and exhibits critical behavior. To understand the implications of the model in Ref. 16, one may consider a plasma with a sufficiently long L_n or L_v and a given seed or noise level of electrostatic waves (acoustic for SRS, Langmuir for SRS) that are sufficiently damped. We define the amount of laser light backscattered by such a seed in terms of its reflectivity R_{seed} . As the averaged intensity I of the beam envelope is increased starting from a value below the onset of instability, the laser reflectivity R sharply increases from R_{seed} once a critical intensity I_c is exceeded. The critical intensity is given approximately by the value of I , at which the linear convective gain ($R/R_{seed} = \exp[G]$) is approximately e^1 over the typical length of a hot spot, $l_{hs} \approx 7f^2\lambda$. This stands in contrast to the value $G = 2\pi$ of the gain exponent customarily taken as the threshold for significant convective instability. According to the model, even if we start with the minimum seed given by thermal density fluctuations (typically $R_{seed} \approx 10^{-8}$), once I increases moderately beyond I_c , then most hot spots undergo pump depletion (all the light is scattered) and R levels off.

We have investigated SRS onsets by varying I and measuring the SRS reflectivity from toroidal hohlraums filled with 1 atm of C_5H_{12} .¹⁸ Figure II-21 shows the results. As with SRS, as I increases above a value I_c (about 10^{14} W/cm² in this case), the SRS reflectivity rises steeply and saturates at about 20%. Figure II-21 includes a fit to the data using the model in Ref. 16. The observed value of I_c for SRS is consistent with our best theoretical estimate.

The concept of a critical intensity for parametric instability seems to be fairly robust in long-scale plasmas. The critical intensity for SRS also has been measured both in the Nova toroidal hohlraums⁷ and in Trident open plasmas.²⁰ The magnitude of I_c for SRS is predicted by the model in Ref. 16 to a reasonable approximation for a variety of plasma conditions.

Large Gas-Filled Hohlraums, $f/4$, Neopentane

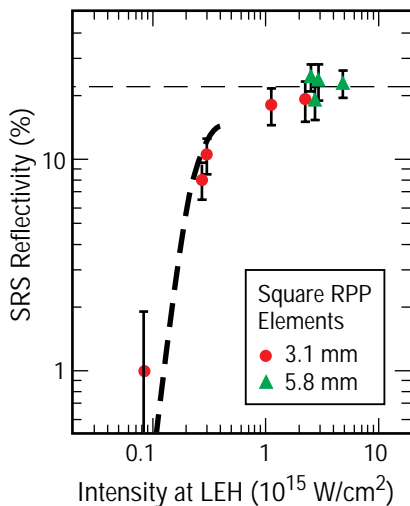


Fig. II-21. A plot of the SRS reflectivity into the interaction-beam cone, integrated over time, versus the interaction-beam intensity at the hohlraum laser entrance hole. The uncertainty in the beam intensity is approximately $\pm 10\%$ of its value.

SRS-Saturation Scaling

We have studied SRS saturation in the toroidal Nova hohlraums. For laser-intensity values similar to those in present NIF designs, it is observed that SRS is in a saturated state so that further increases in laser intensity do not yield a higher beam reflectivity. It is also observed that the SRS reflectivity depends on the damping rate of ion-acoustic waves (IAW), which is normalized to the real ion-acoustic frequency (v_i/ω_i). Because SRS does not involve IAWs directly, this dependence may seem paradoxical. However, SRS can couple to other processes by further parametric decay of the SRS daughter electron-plasma wave, or SRS Langmuir wave (LW). The leading candidate is the Langmuir Decay Instability (LDI), in which the SRS LW further decays into an IAW and another LW,²² as seen experimentally.²³ For a sufficiently strong laser drive, LDI daughter LWs themselves undergo LDI decay, creating so-called Langmuir turbulence. Langmuir turbulence is also relevant to ionospheric plasmas.

The dependence of SRS reflectivity on v_i/ω_i has been studied with various gas fills in toroidal hohlraums, all at 1 atm of pressure and all designed to ionize to $n_e/n_c = 0.11$.²¹ Both v_i and v_e are dominated by collisionless Landau damping for the plasma conditions of interest. In plasmas with multiple ion species, Landau damping of acoustic waves depends on the relative masses of the ions.^{24,25} We have explored this fact, using the hohlraum gas fill, to vary v_i/ω_i in our experiments. Again, C_5H_{12} , C_5D_{12} , CF_4 , and $C_5H_{12} + CF_4$ low-Z gas fills are used.

The time-integrated SRS reflectivity data are shown in Fig. II-22. The data in this figure clearly show that as acoustic damping increases, SRS reflectivity increases. The laser intensity at the LEH is kept in the range of 2×10^{15} to 3.6×10^{15} W/cm². The observed scaling versus v_i is consistent with the linear scaling predicted by a model of SRS saturation by Langmuir turbulence.²⁶

SRS Images

It is very likely that SBS and SRS are spatially and temporally localized within the plasmas we study and do not have smooth, convective growth along the whole path of the laser beam within the plasma. In addition, it appears that SBS and SRS can mutually couple.^{27–31} In order to resolve these issues, it is very desirable to image the scattered light in space and time and thus localize the SRS and SBS processes within the target. We have deployed two optical imaging instruments, the full-aperture-backscatter station imager (FABSI) and the axial imager at the Nova laser, to accomplish this task.^{32,33}

In order to show the potential of SRS imaging as a density diagnostic, we show in Fig. II-23 an image of a conventional methane-filled, cylindrical Nova hohlraum using SRS light from the axial-imager diagnostic. We use the fact that the wavelength of SRS light depends on n_e . This type of hohlraum is used for studies of capsule illumination symmetry,³⁴ although this particular hohlraum has no capsule. The diagnostic was outfitted with a 550- to 650-nm band-pass filter, corresponding to n_e/n_c of 5%–15%. Out of the 2.2-ns pulse,

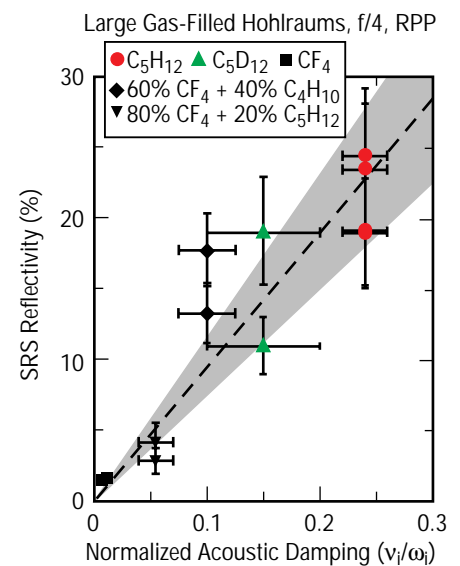
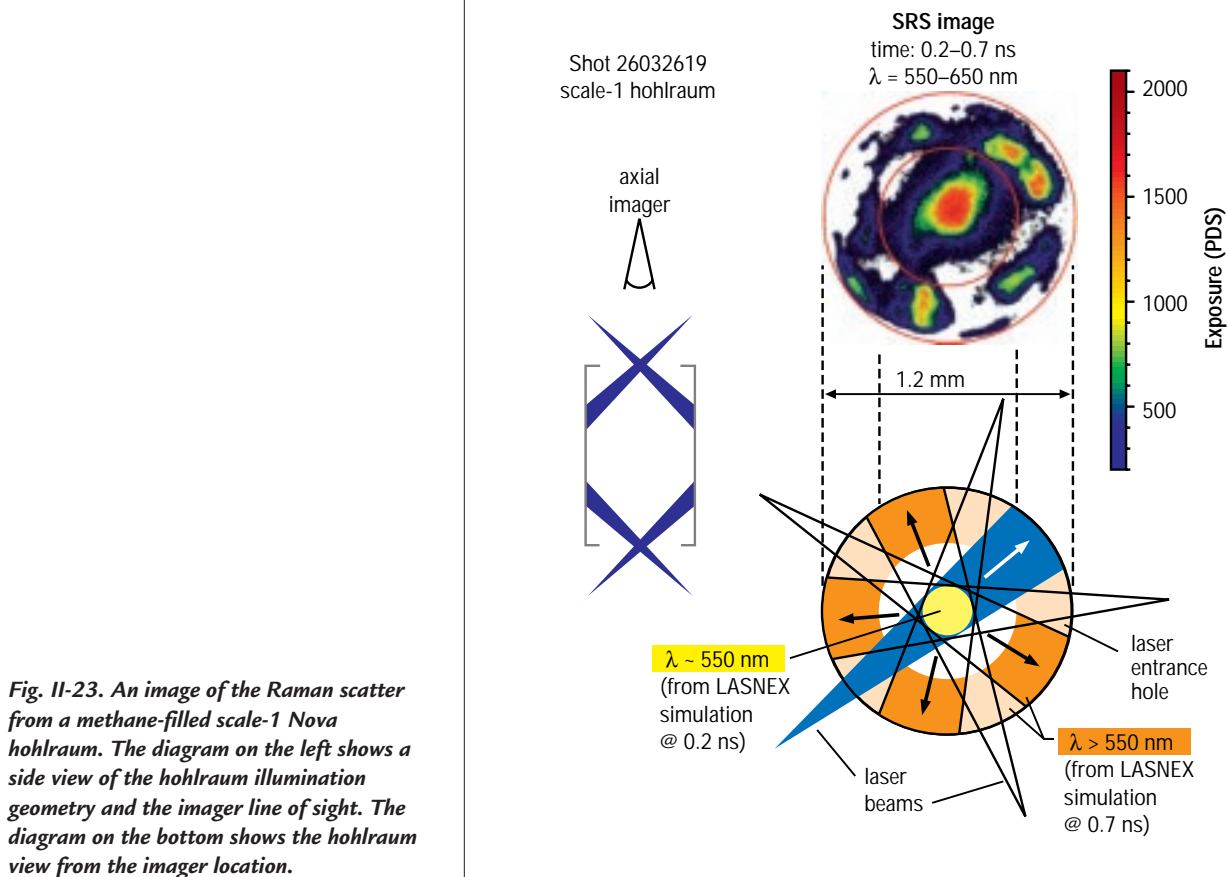


Fig. II-22. Raman backscatter reflectivities of the interaction beam for low-Z hohlraum gas fills. The least-squares linear fit (forced zero intercept) is shown. The shaded area shows the 95% confidence level for the fit.

the frame shown was gated for the 0.2- to 0.7-ns period. The image, when compared with the diagram on the bottom, shows that the LASNEX simulation predicts well the radial location of the $0.05-n_c$ density contour. However, although LASNEX correctly predicts a slight density buildup at the hohlraum axis, the observed density appears to be higher than the LASNEX prediction.

Summary

In summary, the speckled nature of laser beams used in ICF is an important factor in laser-plasma instability processes. For example, models that account for the laser speckles successfully predict the observed onsets of backscattering due to SBS and SRS. Linear convective theory predicts very large levels of SRS backscattering from the long-scale plasmas expected in ignition hohlraums. Our observations of SRS saturation are inconsistent with linear-theory scaling, but are qualitatively understood in terms of other processes. In particular, we have shown direct evidence for the dependence on acoustic damping of the SRS reflectivity. Since SRS itself is unrelated to acoustic waves, this dependence is evidence of other parametric processes determining the nonlinear saturation of Raman backscatter. We have great expectations from optical imaging diagnostics recently deployed at Nova. They could help elucidate important outstanding questions relating to SRS and SRS nonlinear saturation and could also prove to be a valuable density diagnostic.



References

1. J. H. Nuckolls, L. Wood, et al., "Laser Compression of Matter to Super-High Densities: Thermonuclear (CTR) Applications," *Nature* **239**, 139 (1972).
2. J. D. Lindl, R. L. McCrory, and E. M. Campbell, "Progress toward Ignition and Burn Propagation in Inertial Confinement Fusion," *Physics Today* **45:9**, 32 (1992).
3. S. W. Haan, S. M. Pollaine, J. D. Lindl, et al., "Design and Modeling of Ignition Targets for the National Ignition Facility," *Physics of Plasmas* **2**, 2480 (1995).
4. W. J. Krauser, N. M. Hoffman, D. C. Wilson, et al., "Ignition Target Design and Robustness Studies for the National Ignition Facility," *Physics of Plasmas* **3**, 2084 (1996).
5. G. Zimmerman and W. Kruer, "Numerical Simulation of Laser-Initiated Fusion," *Comments on Plasma Physics and Controlled Fusion* **2**, 51 (1975).
6. B. J. MacGowan, B. B. Afeyan, C. A. Back, et al., "Laser-Plasma Interactions in Ignition-Scale Hohlraum Plasmas," *Physics of Plasmas* **3**, 2029 (1996).
7. J. C. Fernández, J. A. Cobble, B. H. Failor, et al., "Dependence of Stimulated Brillouin Scattering on Laser Intensity, Laser f Number, and Ion Species in Hohlraum Plasmas," *Physical Review E* **53**, 2747 (1996).
8. B. H. Wilde, J. C. Fernández, W. W. Hsing, et al., "The Design and Characterization of Toroidal-Shaped NOVA Hohlraums That Simulate National Ignition Facility Plasma Conditions for Plasma Instability Experiments," in *Proceedings of the 12th International Conference on Laser Interaction and Related Plasma Phenomena* (Osaka, Japan, April 1995), *AIP Conference Proceedings* **369:1**, 255 (1996).
9. E. M. Campbell, J. T. Hunt, E. S. Bliss, et al., "Nova Experimental Facility (Invited)," *Review of Scientific Instruments* **57**, 2101 (1986).
10. M. N. Rosenbluth, "Parametric Instabilities in Inhomogeneous Media," *Physical Review Letters* **29**, 565 (1972).
11. M. V. Goldman and D. F. DuBois, "Simulated Incoherent Scattering of Light from Plasmas," *Physics of Fluids* **8**, 1404 (1965).

12. L. M. Gorbunov, "Perturbation of a Medium by a Field of a Strong Electromagnetic Wave," *Soviet Physics JETP* **28**, 1220 (1969).
13. P. E. Young, K. G. Estabrook, W. L. Kruer, et al., "Backscattered Light near the Incident Laser Wavelength from 0.35 μm Irradiated Long Scale Length Plasmas," *Physics of Fluids B* **2**, 1907 (1990).
14. Y. Kato, K. Mima, N. Miyanaga, et al., "Random Phasing of High-Power Lasers for Uniform Target Acceleration and Plasma-Instability Suppression," *Physical Review Letters* **53**, 1057 (1984).
15. H. A. Rose and D. F. DuBois, "Statistical Properties of Laser Hot Spots Produced by a Random Phase Plate," *Physics of Fluids B* **5**, 590 (1993).
16. H. A. Rose and D. F. DuBois, "Laser Hot Spots and the Breakdown of Linear Instability Theory with Application to Stimulated Brillouin Scattering," *Physical Review Letters* **72**, 2883 (1994).
17. V. V. Eliseev, W. Rozmus, et al., "Effect of Diffraction on Stimulated Brillouin Scattering from a Single Laser Hot Spot," *Physics of Plasmas* **3**, 3754 (1996).
18. J. C. Fernández, B. S. Bauer, J. A. Cobble, et al., "Measurements of Laser-Plasma Instability Relevant to Ignition Hohlraums," *Physics of Plasmas* **4**, 1849 (1997).
19. B. B. Afeyan, A. E. Chou, and W. L. Kruer, "New Regimes of Parametric Instabilities in Plasmas with Flat-Topped and Depleted Tail Velocity Distribution Functions," submitted to *Physical Review Letters*.
20. R. G. Watt, J. Cobble, D. F. DuBois, et al., "Dependence of Stimulated Brillouin Scattering on Focusing Optic f Number in Long Scale-Length Plasmas," *Physics of Plasmas* **3**, 1091 (1996).
21. J. C. Fernández, J. A. Cobble, B. H. Failor, et al., "Observed Dependence of Stimulated Raman Scattering on Ion-Acoustic Damping in Hohlraum Plasmas," *Physical Review Letters* **77**, 2702 (1996).
22. D. F. DuBois and M. V. Goldman, "Radiation-Induced Instability of Electron Plasma Oscillations," *Physical Review Letters* **14**, 544 (1965).
23. K. L. Baker, R. P. Drake, B. S. Bauer, et al., "Thomson Scattering Measurements of the Langmuir Wave Spectra Resulting from Stimulated Raman Scattering," *Physical Review Letters* **77**, 67 (1996).

24. H. X. Vu, J. M. Wallace, and B. Bezzerides, "An Analytical and Numerical Investigation of Ion Acoustic Waves in a Two-Ion Plasma," *Physics of Plasmas* **1**, 3542 (1994).
25. E. A. Williams, R. L. Berger, R. P. Drake, et al., "The Frequency and Damping of Ion Acoustic Waves in Hydrocarbon (CH) and the Two-Ion-Species Plasmas," *Physics of Plasmas* **2**, 129 (1995).
26. B. Bezzerides, D. F. DuBois, and H. A. Rose, "Saturation of Stimulated Raman Scattering by the Excitation of Strong Langmuir Turbulence," *Physical Review Letters* **70**, 2569 (1993).
27. C. J. Walsh, D. M. Villeneuve, and H. A. Baldis, "Electron Plasma-Wave Production by Stimulated Raman Scattering: Competition with Stimulated Brillouin Scattering," *Physical Review Letters* **53**, 1445 (1984).
28. H. A. Rose, D. F. DuBois, and B. Bezzerides, "Nonlinear Coupling of Stimulated Raman and Brillouin Scattering in Laser-Plasma Interactions," *Physical Review Letters* **58**, 2547 (1987).
29. D. M. Villeneuve, H. A. Baldis, and J. E. Bernard, "Suppression of Stimulated Raman Scattering by the Seeding of Stimulated Brillouin Scattering in a Laser-Produced Plasma," *Physical Review Letters* **59**, 1585 (1987).
30. H. A. Baldis, P. E. Young, R. P. Drake, et al., "Competition between the Stimulated Raman and Brillouin Scattering Instabilities in 0.35- μm Irradiated CH Foil Targets," *Physical Review Letters* **62**, 2829 (1989).
31. D. S. Montgomery, B. B. Afeyan, B. J. MacGowan, et al., "Persistent Anti-Correlation of Stimulated Raman and Brillouin Scattering Levels in Laser-Produced Plasmas," submitted to *Physical Review Letters*.
32. J. C. Fernández, R. R. Berggren, K. S. Bradley, et al., "Improved Optical Diagnostics for the NOVA Laser," *Review of Scientific Instruments* **66**, 626 (1995).
33. M. D. Wilke, J. C. Fernández, R. R. Berggren, et al., "Full Aperature Backscatter Station Imager Diagnostic System for Far-Field Imaging of Laser-Plasma Instabilities at Nova," *Review of Scientific Instruments* **68**, 672 (1997).
34. N. D. Delamater, T. J. Murphy, A. A. Hauer, et al., "Symmetry Experiments in Gas-Filled Hohlräume at NOVA," *Physics of Plasmas* **3**, 2022 (1996).